THE JOURNAL OF PHYSICAL CHEMISTRY A
A JOURNAL OF THE AMERICAN CHEMICAL SOCIETY

pubs.acs.org/JPCA Article

F12-TZ-cCR: A Methodology for Faster and Still Highly Accurate Quartic Force Fields

Alexandria G. Watrous, Brent R. Westbrook, and Ryan C. Fortenberry*

Cite This: J. Phys. Chem. A 2021, 125, 10532−10540 Read Online

ACCESS | Metrics & More | Article Recommendations | Supporting Information

ABSTRACT: The F12-TZ-cCR quartic force field (QFF) methodology, defined here as CCSD(T)-F12b/cc-pCVTZ-F12 with further corrections for relativity, is introduced as a cheaper and even more accurate alternative to more costly composite QFF methods like those containing complete basis set extrapolations within canonical coupled cluster theory. F12-TZ-cCR QFFs produce B_0 and C_0 vibrationally averaged principal rotational constants within 7.5 MHz of gas-phase experimental values for tetraatomic and larger molecules, offering higher accuracy in these constants than the previous composite methods. In addition, F12-TZ-cCR offers an order of magnitude decrease in the computational cost of highly accurate QFF methodologies accompanying this increase in accuracy. An additional order of magnitude in cost reduction is achieved in the F12-DZ-cCR method, while also matching the accuracy of the traditional composite method's B_0 and C_0 constants. Finally, F12-DZ and F12-TZ are benchmarked on the same test set, revealing that both methods can provide anharmonic vibrational frequencies that are comparable in accuracy to all three of the more expensive methodologies, although their rotational constants lag behind. Hence, the present work demonstrates that highly accurate theoretical rovibrational spectral data can be obtained for a fraction of the cost of conventional QFF methodologies, extending the applicability of QFFs to larger molecules.

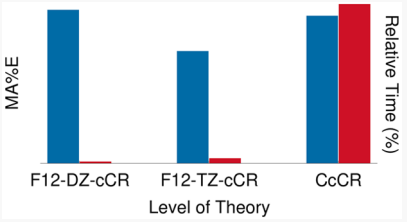

INTRODUCTION

One of the most effective tools[1−6] for computing efficient theoretical rovibrational spectral data is the quartic force field (QFF) combined with vibrational perturbation theory at second order (VPT2).[7−9] QFFs are fourth-order Taylor series expansions of the internuclear potential energy portion of the Watson Hamiltonian.[10] VPT2 allows such a local potential energy surface (PES) to serve as the basis for the generation of reliable anharmonic rovibrational spectral data without the high cost of a more global PES. An often-employed and highly accurate QFF methodology is a composite method based on coupled cluster theory at the singles, doubles, and perturbative triples [CCSD(T)] level[11−13] and is known as CcCR. The "C" stands for a complete basis set (CBS) extrapolation, the "cC" stands for core correlation, and the "R" stands for relativity.[14] The CBS extrapolation in CcCR uses a three-point extrapolation formula with the aug-cc-pVTZ, aug-cc-pVQZ, and aug-cc-pV5Z basis sets[15−18] with additional tight d functions included for the third row elements. The triple-ζ Martin−Taylor (MT) core electron basis set[19] is used to correct for the effects of core correlation, while the Douglas−Kroll (DK) Hamiltonian[20,21] and associated triple-ζ basis set[15,22] are used to correct for scalar relativistic effects. In both cases, the correction is computed by taking the difference between computations with and without the factor in question enabled.

The CcCR methodology, again combined with VPT2, frequently yields fundamental vibrational frequencies within 5.0 cm^{-1} of gas-phase experimental data and often within 1.0 cm^{-1}.[10,23−33] Similarly, agreement with gas-phase B_0 and C_0 vibrationally averaged principal rotational constants has recently been shown to be as good as 20 MHz.[34] Despite this success, even better performance in the rotational constants is necessary to maximize the predictive power of these computations. In addition, the great computational cost of CcCR has thus far limited its application to molecules of roughly five atoms and fewer, making it unusable for larger, astronomically relevant molecules like polycyclic aromatic hydrocarbons (PAHs).

On the other hand, explicitly correlated CCSD(T) methods such as CCSD(T)-F12b[35,36] with the corresponding cc-pVTZ-F12 basis sets,[37,38] the combination of which is often termed F12-TZ, can generate QFFs that are much less expensive than CcCR for some sacrifice of accuracy. F12-TZ QFFs plus VPT2 typically produce fundamental vibrational frequencies within 5−7 cm^{-1} of gas-phase experiment.[34] However, the rotational constants produced are even less accurate than those of CcCR, primarily because of the lack of core electron correlation. Such correlation is necessary to produce accurate bond lengths in coupled cluster computations. This makes F12-TZ a less

Received: September 22, 2021
Revised: November 15, 2021
Published: November 30, 2021

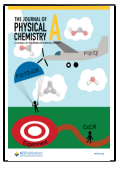

https://doi.org/10.1021/acs.jpca.1c08355
J. Phys. Chem. A 2021, 125, 10532−10540

favorable choice for computing rotational data. Thus, a better method is needed that produces more accurate rotational constants than F12-TZ but is faster than CcCR.

A candidate for such a method is one that replaces the expensive CBS extrapolation in CcCR with the explicit correlation found in the F12-TZ wave function. As early as 2010, explicitly correlated methods were predicted to be fast and accurate enough to replace the CBS extrapolation in the near future.[39] In line with this prediction, advancements in the aforementioned F12 methods should allow them to take the place of the CBS extrapolation and reduce the cost of the QFF. In addition, incorporating the core correlation correction directly into the F12 method and using the corresponding cc-pCVTZ-F12 basis set[40] allow that separate portion of the composite energy to be omitted. Combining this approach with the same, inexpensive correction for scalar relativity used in CcCR yields what will hereafter be termed the F12-TZ-cCR methodology.

Additionally, previous work has shown that even CCSD(T)-F12 with a double-ζ basis set can give reasonable harmonic[41] and fundamental[42,43] vibrational frequencies for certain molecules. As such, the present work also seeks to benchmark the use of F12-DZ and F12-DZ-cCR for both vibrational frequencies and vibrationally averaged principal rotational constants since these will lead to even greater speedups relative to CcCR. Such speedups will be necessary to lend theoretical support to NASA missions such as the ongoing *Stratospheric Observatory for Infrared Astronomy* (SOFIA) and the upcoming *James Webb Space Telescope* (JWST), especially for predictions of the spectra of molecules larger than five atoms, such as the aforementioned PAHs.

COMPUTATIONAL DETAILS

The CcCR QFFs begin with optimizing the geometry at the CCSD(T)/aug-cc-pV5Z level for the closed-shell systems and the ROHF-UCCSD(T)/aug-cc-pV5Z level[44] for the open-shell molecules. These are both hereafter termed "5Z". The geometrical parameters are then corrected by adding the difference between those calculated by using MT basis sets with (MTc) and without (MT) core electrons enabled:

$$R_{\mathrm{CcCR}} \equiv R_{5Z} + (R_{\mathrm{MTc}} - R_{\mathrm{MT}}) \tag{1}$$

For the F12-*XZ* methods, where *X* is D or T, the geometrical parameters are optimized at the UCCSD(T)-F12b[36] or CCSD(T)-F12b/cc-pV*XZ*-F12[37,39,45] level of theory, while for the F12-*XZ*-cCR methods, where *X* is again D or T, the optimizations use the cc-pCV*XZ*-F12 basis sets with treatment of inner- and outer-core electrons enabled. All of these calculations use the Molpro 2020.1 software package.[46]

After the optimizations, each geometry is displaced by 0.005 Å or 0.005 radians to construct the QFFs.[47] For each CcCR displacement, the total single-point energies are computed as combinations of the seven component energies shown below:

$$E_{\mathrm{CcCR}} \equiv E_{\mathrm{CBS}} + \Delta_{\mathrm{cC}} + \Delta_{\mathrm{R}} \tag{2}$$

where E_{CBS} is the energy of the three-point TQ5 CBS extrapolation[10,18] given by

$$E(l) \equiv A + B(l + 1/2)^{-4} + C(l + 1/2)^{-6} \tag{3}$$

in which *A*, *B*, and *C* are the energies from the 5Z, QZ, and TZ basis set computations, respectively, and *l* is the highest angular momentum function included in the basis set.[10] Δ_{cC} and Δ_{R} are given by

$$\Delta_{\mathrm{cC}} \equiv E_{\mathrm{MTc}} - E_{\mathrm{MT}} \tag{4}$$

and

$$\Delta_{\mathrm{R}} \equiv E_{\mathrm{DKr}} - E_{\mathrm{DK}} \tag{5}$$

E_{DKr} is the energy computed by using the DK basis set with relativity enabled, and E_{DK} is the corresponding energy with relativity disabled.

Similarly, the F12-*XZ*-cCR single-point energies are composed of the CCSD(T)-F12b/cc-pCV*XZ* (C*XZ*) base energy and the same, canonical CCSD(T) correction for scalar relativity as in CcCR, as shown below:

$$E_{\mathrm{XZ\text{-}cCR}} \equiv E_{\mathrm{CXZ}} + \Delta_{\mathrm{R}} \tag{6}$$

For the F12-TZ-cCR QFFs, triple-ζ basis sets are used for both the base energy computation and for the scalar relativity correction, while the corresponding double-ζ basis sets are used for both parts of the F12-DZ-cCR QFFs.

The F12-*XZ* QFFs are solely composed of the F12-*XZ* energies. In all cases, the resulting energies are then fit by a least-squares procedure to yield the equilibrium geometry. A refit of the PES to the minimum of the function determined by the least-squares fit zeroes the gradients and gives the new equilibrium geometry and the corresponding force constants. The force constants are then converted from symmetry-internal coordinates (SICs) to Cartesian coordinates by using the INTDER program.[48] The SPECTRO software package[49] uses the Cartesian force constants in VPT2[7,8] and second-order rotational perturbation theory[50] to calculate rovibrational spectral data. Type 1 and 2 Fermi resonances and Fermi polyads,[51] Coriolis resonances, and Darling−Dennison resonances are taken into account[51,52] to further increase the accuracy of the resulting rovibrational data.

To combat the well-known out-of-plane bending (OPB) problem,[53] larger step sizes of 0.010 rad are used for the out-of-plane coordinates of *c*-C_3H_2, namely the torsional coordinates of the terminal hydrogens. Similarly, a larger step size of 0.010 Å or rad is used for all three SICs of HSO because of the larger atomic size of sulfur.

The F12-*XZ*, F12-*XZ*-cCR, and CcCR QFFs calculated herein are benchmarked against available, high-resolution gas-phase experimental data. The citations for these literature values are presented in Table 1. The molecules chosen for this work are a mixture of closed-shell and radicals to give a diverse test set. The size of the molecules examined has been limited by the availability of experimental data and the tractability of CcCR computations.[34] The vibrationally averaged principal rotational constants and vibrational frequencies are reported relative to known experimental data by subtracting the experimental results from the computed values. The timing of each method is reported as the percentage of the CcCR wall time. The absolute timing information is reported in Table S1 of the Supporting Information. Harmonic vibrational frequencies and the full set of fundamental vibrational frequencies can be found in Tables S2 and S3. In all of the tables, the mean absolute error (MAE), or unsigned average, is calculated by subtracting the experimental values from the computed values and averaging their absolute values. Similarly, the mean absolute percent errors (MA%Es) are computed by averaging these differences relative to the experimental values.

https://doi.org/10.1021/acs.jpca.1c08355
J. Phys. Chem. A 2021, 125, 10532−10540

Table 1. Literature Citations for Experimental Data

molecule	vibrational frequencies[a]	rotational constants
C_2H^-		54
H_2CO	55	56
H_2O	57	58
HCN	59	59
HCO^+	60−62	63
HMgNC		64
HNC	65	65
HNO	66	66
HSO	67	68
HSS	69	70
HOCN	71	72
c-HOCO		73
t-HOCO	74	73
$HOCO^+$	75	76
HPSi		77
NH_2^-	78	78
NH_3	55	79, 80
$NNOH^+$	81	82
c-C_3H_2	83	84

[a]Blank spaces represent molecules without available experimental vibrational frequencies.

RESULTS AND DISCUSSION

Accuracy. The F12-TZ-cCR methodology produces highly accurate vibrationally averaged principal rotational constants relative to gas-phase experiment, as shown in Table 2. Whereas the current gold-standard method, CcCR, has an MAE difference from experiment of 555.6 MHz, F12-TZ-cCR achieves a slightly higher MAE difference of 690.1 MHz but for a minute fraction of the computational cost. Comparing the two in relative terms, F12-TZ-cCR differs from experiment by 0.19% on average compared to the 0.25% of CcCR, suggesting F12-TZ-cCR is actually closer to experiment by this metric. Regardless, neither of these criteria suggests either method is usable for predicting rotational constants because of their massive deviation from the experimental values. However, a large portion of the error is due to the A_0 constants, which are well-known to cause such issues in this type of analysis.[34] While A_0 constants are always larger than B_0 and C_0, the near-prolate nature of many of the molecules in the current test set means that the A_0 constants can be orders of magnitude larger. In turn, this means that a small relative error can lead to massive absolute errors in these constants. Thus, Table 3 shows the same statistics after removing the A_0 rotational constants.

Reducing the data set to only the B_0 and C_0 constants gives MAEs of 97.5 and 81.7 MHz for CcCR and F12-TZ-cCR, respectively, which are much more reasonable. The MA%E values also improve without A_0 to 0.20% and 0.10%, respectively, suggesting that the large magnitude of these constants is not the only factor contributing to their absolute inaccuracy, but the magnitude still accounts for much of the error. Despite the order-of-magnitude improvement in the performance when only considering the B_0 and C_0 constants, even 80 MHz is not sufficient for aiding experimental detection. Looking at the errors in B_0 and C_0 reported in Table 2, some molecules can be identified as potential outliers. Chief among these are the same molecules excluded in previous work on benchmarking CcCR itself,[34] namely H_2O, NH_2^-, and NH_3. Excluding these from the statistics brings the F12-TZ-cCR MAE to 22.9 MHz (0.09%) and that of CcCR to 47.8 MHz (0.21%). This F12-TZ-cCR MAE is nearly lower than the previous CcCR result of 18.9 MHz, which required excluding all triatomics in addition to NH_3. Discarding the triatomics and NH_3 here gives F12-TZ-cCR an MAE of 7.5 MHz (0.05%), which is tantalizingly close to the accuracy needed to lend computational support for experimental investigations. More importantly, however, this is considerably lower than the corresponding CcCR difference of 24.2 MHz or 0.17%.

As anticipated, the performance of the F12-TZ QFFs is much less impressive, yielding an overall MAE of 986.5 MHz (0.59%) and 163.3 MHz (0.59%) in the B_0 and C_0 constants and 61.7 MHz (0.49%) in the case without NH_3 and the triatomic molecules. The F12-DZ QFFs yield slightly worse absolute results still with corresponding values of 1150.3, 177.8, and 73.9 MHz, but the relative values of 0.57, 0.53, and 0.58% improve slightly, at least for the first two cases. The addition of the cCR corrections gives F12-DZ-cCR performance intermediate to F12-TZ and F12-TZ-cCR with MAE differences of 870.0, 125.6, and 16.6 MHz relative to experiment (0.26, 0.18, and 0.13%). This suggests that even F12-DZ-cCR produces more accurate B_0 and C_0 rotational constants than CcCR for tetra-atomic and larger molecules.

Similar trends are borne out in the vibrational data shown in Table 4. Unlike the vibrationally averaged principal rotational constants, all of which have comparable gas-phase experimental data, only a relatively small subset of the computed vibrational frequencies have directly comparable laboratory results. Only these are presented in Table 4 as differences from the experimental values, while the full set of computed fundamental frequencies is shown in Table S3. CcCR performs slightly better on average than F12-TZ-cCR for the fundamental vibrational frequencies, attaining an MAE difference of 6.3 cm^{-1} compared to the 8.6 cm^{-1} MAE of F12-TZ-cCR. Conventional F12-TZ comes close to both of these with an MAE of 8.8 cm^{-1}. Somewhat surprisingly, F12-DZ actually has the second lowest overall MAE of the molecules and methods tested at 7.0 cm^{-1}. This agrees with previous work[43,85] showing that F12-DZ is comparably accurate to F12-TZ, but both F12-*X*Z methods are performing very well relative to CcCR for this test set. F12-DZ-cCR, in contrast, performs a bit worse than any of the other methods, with an MAE of 13.8 cm^{-1}. Given the surprising performance of both double-ζ methods, the specific success of F12-DZ in this case is likely due to some fortuitous cancellation of errors that is disrupted upon the introduction of the core correlation and relativity corrections. Nevertheless, all five levels of theory can compute anharmonic vibrational frequencies with a reasonable level of accuracy.

Timing. Given the similarity of the vibrational results across the board and the rotational results between F12-TZ-cCR and CcCR, some criterion is needed to differentiate the two. The most obvious factor is the computational cost. Table 5 shows the wall time of each QFF as a percentage of the CcCR time. CcCR is not shown since in every molecular test case its value is 100%. Like Tables 2 and 4, the average of each column is shown at the bottom. Looking at these averages, any of these methods are clearly preferable to CcCR when time is of the essence. On average, even the second most expensive method, F12-TZ-cCR, takes 3.05% of the time of CcCR. Even in the worst case of HSS, the F12-TZ-cCR QFF took less than 10% of the time of the CcCR QFF, suggesting that F12-TZ-cCR

https://doi.org/10.1021/acs.jpca.1c08355
J. Phys. Chem. A 2021, 125, 10532−10540

Table 2. Difference in Principal Rotational Constants Relative to Experiment (in MHz)

molecule	const	F12-DZ	F12-TZ	F12-DZ-cCR	F12-TZ-cCR	CcCR	experiment
C_2H^-	*B*	−191.6	−174.8	5.6	43.1	55.5	41639.237
H_2CO	*A*	−129.4	−175.5	618.5	595.0	746.6	281970.5406
H_2CO	*B*	−135.2	−117.2	−26.6	18.8	57.3	38836.05038
H_2CO	*C*	−107.2	−94.4	−12.9	21.4	53.1	34002.19978
H_2O	*A*	−8076.4	−6742.3	−5924.8	−4589.2	−1814.2	835840.29
H_2O	*B*	102.3	−487.8	397.9	−16.3	161.7	435351.72
H_2O	*C*	−321.9	−421.7	41.1	15.8	399.1	278138.7
HCN	*B*	−189.3	−159.6	−18.6	36.6	66.8	44316.009
HCO^+	*B*	−192.5	−163.6	−50.3	12.6	59.3	44594.42866
HMgNC	*B*	−74.3	−69.9	−5.4	−5.3	−12.1	5481.49
HNC	*B*	−205.5	−183.7	−23.8	24.1	56.6	45331.9827
HNO	*A*	3510.3	4443.1	5123.7	6132.3	6919.6	553898.62
HNO	*B*	−53.5	−50.8	19.3	77.5	117.8	42312.8124
HNO	*C*	−47.2	−40.5	23.3	78.1	116.5	39165.1415
HSO	*A*	519.1	217.6	524.4	425.6	963.0	299483.9
HSO	*B*	23.8	18.2	21.9	70.8	132.4	20502.7847
HSO	*C*	21.8	15.8	20.3	62.4	118.3	19135.6989
HSS	*A*	1040.5	−1012.5	1330.9	854.4	1199.1	296974.403
HSS	*B*	−35.3	−217.0	−31.4	3.3	18.8	7996.378
HSS	*C*	−32.7	−206.2	−28.8	3.7	18.6	7776.723
HOCN	*A*	−1596.8	−610.7	224.3	1291.6	2864.2	674308.0
HOCN	*B*	−48.4	−37.9	−13.8	4.7	13.2	10577.0138
HOCN	*C*	−46.9	−36.5	−13.0	5.1	13.8	10398.4918
c-HOCO	*A*	−788.9	−576.0	−191.1	−18.9	−375.0	142944.9287
c-HOCO	*B*	−47.4	−36.4	−16.7	6.4	29.9	11739.4855
c-HOCO	*C*	−45.1	−34.6	−15.5	5.0	23.0	10830.1428
t-HOCO	*A*	−892.0	−492.2	34.4	500.6	584.3	167768.064
t-HOCO	*B*	−46.5	−35.5	−12.1	2.0	16.2	11433.322
t-HOCO	*C*	−44.2	−32.9	−10.2	3.9	16.6	10686.63
$HOCO^+$	*A*	−16284.2	−12448.6	−12090.2	−8433.7	−5247.4	789951.1452
$HOCO^+$	*B*	−49.1	−38.7	−16.5	2.0	13.6	10773.7341
$HOCO^+$	*C*	−48.4	−37.7	−16.1	2.5	14.4	10609.4312
HPSi	*A*	−184.4	−1396.1	1240.0	590.3	−91.1	297187.0
HPSi	*B*	−66.8	−62.3	−23.7	6.0	0.3	8169.95742
HPSi	*C*	−60.8	−57.4	−18.9	8.8	2.7	7936.6581
NH_2^-	*A*	−8414.8	−7442.5	−5975.4	−4745.9	−997.7	691045.5991
NH_2^-	*B*	1670.8	672.8	2062.9	1254.8	383.0	391780.7758
NH_2^-	*C*	−108.5	−380.4	353.0	188.4	291.4	243270.4873
NH_3	*A*	−2128.3	−2051.6	−1066.1	−1022.0	−567.1	298107.0248
NH_3	*C*	599.3	439.8	675.4	637.6	693.7	185751.407
$NNOH^+$	*A*	−4156.7	−2691.2	−2870.8	−729.8	798.5	625957.716
$NNOH^+$	*B*	−46.6	−31.6	−18.3	9.1	19.8	11301.5628
$NNOH^+$	*C*	−45.3	−30.4	−17.7	9.4	20.2	11084.28
c-C_3H_2	*A*	−234.0	−198.6	−45.8	24.5	65.2	35092.5964
c-C_3H_2	*B*	−151.2	−135.2	−26.7	8.5	29.5	32212.9312
c-C_3H_2	*C*	−98.9	−86.5	−22.2	3.4	18.5	16749.3147
SiC_2	*A*	−235.8	−238.5	34.3	61.0	111.6	52473.66
SiC_2	*B*	−136.3	−111.1	−65.7	−8.1	−17.4	13158.654
SiC_2	*C*	−98.4	−79.9	−41.7	0.5	−3.0	10441.619
	avg	−844.7	−749.5	−349.4	−150.6	159.5	
	MAE	1150.3	986.5	870.0	690.1	555.6	

gives at least an order-of-magnitude speedup, while also providing more accurate vibrationally averaged principal rotational constants and equally accurate vibrational frequencies.

Figures 1 and 2 graphically summarize all of these results. In both cases, the right axis corresponds to the percentage of the CcCR wall time required for each method and the left axis to the MA%E for each method. As described above, F12-TZ-cCR has the smallest percentage error relative to the experimental rotational constants, while all five methods have MA%Es less than 2% for the fundamental frequencies. All three methods including a treatment of core correlation and scalar relativity show much better performance in the rotational constants compared to F12-DZ and F12-TZ, suggesting that accounting for these effects is necessary for accurate rotational spectra.[23,86] In contrast, there is virtually no difference in the vibrational

https://doi.org/10.1021/acs.jpca.1c08355
J. Phys. Chem. A 2021, 125, 10532−10540

Table 3. Summary of Principal Rotational Constant MAEs and MA%Es Relative to Experiment

set	units	F12-DZ	F12-TZ	F12-DZ-cCR	F12-TZ-cCR	CcCR
A_0, B_0, and C_0	MHz	1150.3	986.5	870.0	690.1	555.6
	%	0.57	0.59	0.26	0.19	0.25
B_0 and C_0	MHz	177.8	163.3	125.6	81.7	97.5
	%	0.53	0.59	0.18	0.10	0.20
B_0 and C_0 without H_2O, NH_2^-, and NH_3	MHz	111.8	108.6	25.5	22.9	47.8
	%	0.59	0.66	0.17	0.09	0.21
B_0 and C_0 without triatomics and NH_3	MHz	73.9	61.7	16.6	7.5	24.2
	%	0.58	0.49	0.13	0.05	0.17
A_0	MHz	3354.7	2852.6	2557.4	2069.1	1594.1
	%	0.67	0.59	0.46	0.38	0.35
ν_x	cm^{-1}	7.0	8.8	13.8	8.6	6.3
	%	1.15	1.84	1.12	1.30	0.66

Table 4. Difference in Fundamental Vibrational Frequencies Relative to Experiment (in cm^{-1})

molecule	mode	F12-DZ	F12-TZ	F12-DZ-cCR	F12-TZ-cCR	CcCR	expt
H_2CO	1	3.1	−16.4	14.6	10.6	−9.3	2843.1
H_2CO	2	−7.1	−3.8	−0.6	−0.3	1.7	2782.5
H_2CO	3	1.9	1.7	5.2	5.9	6.6	1746.1
H_2CO	4	1.4	−0.5	6.7	1.6	2.6	1500.1
H_2CO	5	−2.3	−1.8	8.8	−0.7	2.2	1249.1
H_2CO	6	−5.0	0.0	10.3	0.0	3.2	1167.3
H_2O	1	0.2	−2.7	2.9	−0.0	3.7	3755.929
H_2O	2	4.1	−0.6	6.4	1.7	4.7	3657.053
H_2O	3	6.8	4.1	6.3	5.9	3.7	1594.746
HCN	1	−3.9	−6.0	0.2	−0.3	1.3	3311.47
HCN	2	0.4	0.3	5.0	8.6	9.7	2096.84
HCN	3	4.5	1.7	2.0	2.7	5.6	711.97
HCO^+	1	−3.7	−5.9	−1.7	−2.3	0.2	3088.73951
HCO^+	2	−4.8	−2.5	0.9	3.8	6.6	2183.9496
HCO^+	3	−0.8	0.1	0.9	−4.3	2.2	829.721
HNC	1	−6.2	−6.2	−0.2	−1.0	1.2	3652.65
HNC	2	−6.0	−4.5	1.8	5.0	5.3	2023.86
HNC	3	−6.9	−3.3	5.8	0.1	8.8	462.72
HNO	1	−18.5	−18.3	−39.3	−12.5	−10.4	2683.9521
HNO	2	7.7	7.7	−7.6	12.0	11.8	1565.3481
HNO	3	−0.9	10.7	−16.2	12.6	9.7	1500.8192
HSO	1	9.9	19.8	7.7	11.7	14.5	2325.1
HSO	2	12.1	16.7	10.4	16.2	11.8	1080.4
HSO	3	−1.1	5.6	5.8	−19.7	4.2	1013.9
HSS	3	7.0	−21.1	−9.6	−2.1	6.4	596.27996
HOCN	2	−18.1	−6.7	−4.5	2.3	0.6	2302.0
t-HOCO	1	1.4	−1.9	16.3	26.2	−12.6	3635.702
t-HOCO	2	2.0	2.4	276.2	30.9	11.6	1852.567
$HOCO^+$	1	−2.1	−5.0	11.0	−1.8	−0.3	3375.37426
NH_2^-	1	−1.6	0.1	4.5	4.0	5.9	3190.291
NH_2^-	2	6.3	4.2	10.4	6.9	5.8	3121.9306
NH_3	1	2.5	2.1	7.1	8.3	8.9	3337.0
NH_3	2	45.5	30.8	7.6	26.5	24.4	950.0
NH_3	3	−3.5	−8.6	0.5	−0.9	1.5	3444.0
NH_3	4	2.8	1.4	1.6	3.1	1.5	1627.0
$NNOH^+$	1	0.8	0.9	3.1	1.1	3.9	3330.9107
c-C_3H_2	4	−4.1	−1.7	0.9	22.3	0.1	1277.371132
SiC_2	1	−6.8	−11.1	2.5	2.4	4.7	1746.0
SiC_2	2	0.9	6.7	4.3	−4.7	4.0	840.6
SiC_2	3	−59.6	−111.0	−30.6	−67.9	−21.6	196.37
	avg	−1.0	−3.1	8.4	2.8	3.7	
	MAE	7.0	8.8	13.8	8.6	6.3	

performance between F12-DZ and F12-DZ-cCR, while there is a noticeable but likely statistically insignificant difference between the MA%E of F12-TZ and F12-TZ-cCR. Looking at the relative MAEs shown in Figure 2 also shows F12-DZ and

https://doi.org/10.1021/acs.jpca.1c08355
J. Phys. Chem. A 2021, 125, 10532−10540

Table 5. Timing as a Percentage of the CcCR Wall Time (%)

molecule	F12-DZ	F12-TZ	F12-DZ-cCR	F12-TZ-cCR
C_2H^-	0.73	2.90	1.49	3.84
H_2CO	0.05	0.20	0.08	0.59
H_2O	1.49	4.62	2.80	4.30
HCN	0.76	2.51	1.54	3.94
HCO^+	0.79	3.36	1.62	4.09
HMgNC	0.05	0.42	1.33	1.72
HNC	0.78	3.26	1.53	3.87
HNO	0.30	1.36	0.81	2.94
HSO	0.40	1.41	2.14	6.15
HSS	0.20	9.90	1.47	9.00
HOCN	0.05	0.13	0.08	0.52
c-HOCO	0.09	0.38	0.34	1.64
t-HOCO	0.13	0.39	0.21	1.67
$HOCO^+$	0.03	0.14	0.05	0.37
HPSi	0.13	0.41	0.66	4.17
NH_2^-	1.24	2.97	2.45	4.28
NH_3	0.06	0.12	0.13	0.18
$NNOH^+$	0.04	0.27	0.12	0.87
SiC_2	0.28	0.70	0.72	3.82
avg	0.40	1.87	1.03	3.05

F12-DZ-cCR performing surprisingly better than the triple-ζ QFFs, despite F12-DZ-cCR having a worse performance in terms of the absolute MAEs. This serves to further emphasize the similarity of all five methods. What does not change is the fact that CcCR is immensely costly for its relative accuracy in both the vibrationally averaged principal rotational constants and the vibrational frequencies. On a similar note, exploratory calculations have been undertaken to extend the analysis to the F12-QZ and F12-QZ-cCR levels, but these results are only comparable in accuracy to the triple-ζ results for a disproportionate increase in cost that made them only slightly faster than CcCR.

CONCLUSIONS

This work presents F12-TZ-cCR, a new, highly accurate composite QFF methodology for the computation of vibrationally averaged principal rotational constants and fundamental vibrational frequencies. This method produces comparably accurate anharmonic frequencies to and more accurate rotational constants than the previous gold-standard method, CcCR. In particular, F12-TZ-cCR achieves an average deviation from experimental rotational constants of only 7.5 MHz (0.05%) for tetra-atomic and larger molecules. This is an 11.4 MHz improvement relative to the previously reported performance of CcCR on the same test set.[34] More important, however, is the fact that such performance is achieved simultaneously with an order of magnitude decrease in the cost of computing the QFFs. As such, F12-TZ-cCR should be preferred to CcCR for all future QFFs requiring a high degree of accuracy. If time cost is of the utmost concern, even F12-DZ-cCR should perform better than CcCR in many cases and afford an additional, albeit modest, increase in efficiency relative to F12-TZ-cCR.

While F12-DZ-cCR and F12-TZ-cCR QFFs will already allow for the accurate study of much larger molecules than CcCR, the present work also offers more evidence for how well F12-DZ QFFs can perform. For fundamental frequencies, in particular, these QFFs perform as well as, if not better than, the cCR QFFs, suggesting that another order of magnitude speedup can be gained by using F12-DZ when vibrational frequencies are the primary data of interest. The same is not true if accurate rotational constants are required, since the core correlation corrected QFFs perform much better in that case. But for large, astronomically relevant molecules like mineral precursors[87] and PAHs,[88] F12-DZ is an excellent choice. PAHs, in particular, are an appealing use-case for F12-DZ since their nonpolarity means they are not observable by pure rotational spectroscopy anyway. Overall, the methods presented herein offer a framework for extending the purview of highly accurate theoretical rovibrational analysis to larger molecules than have ever been examinable before. Such

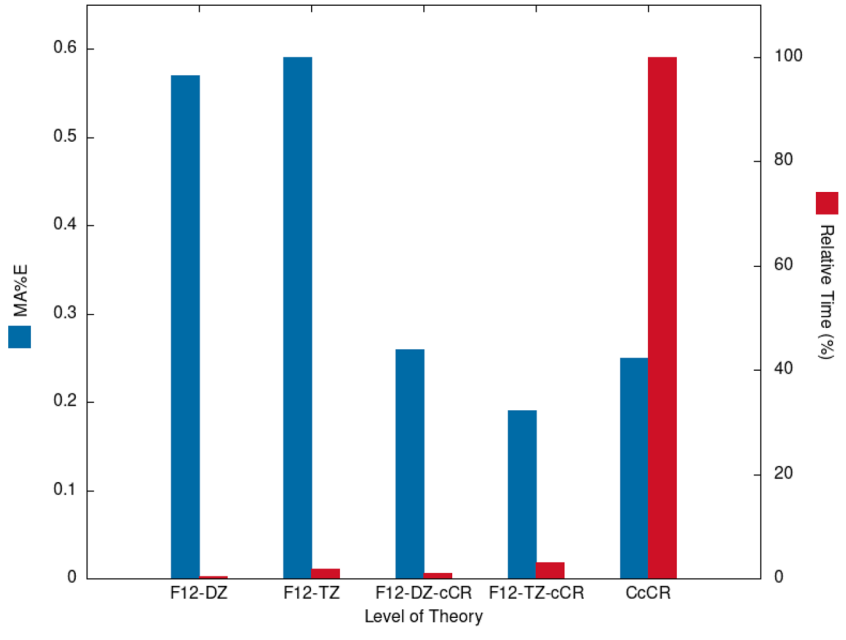

Figure 1. MA%E in the principal rotational constants and timing.

https://doi.org/10.1021/acs.jpca.1c08355
J. Phys. Chem. A 2021, 125, 10532−10540

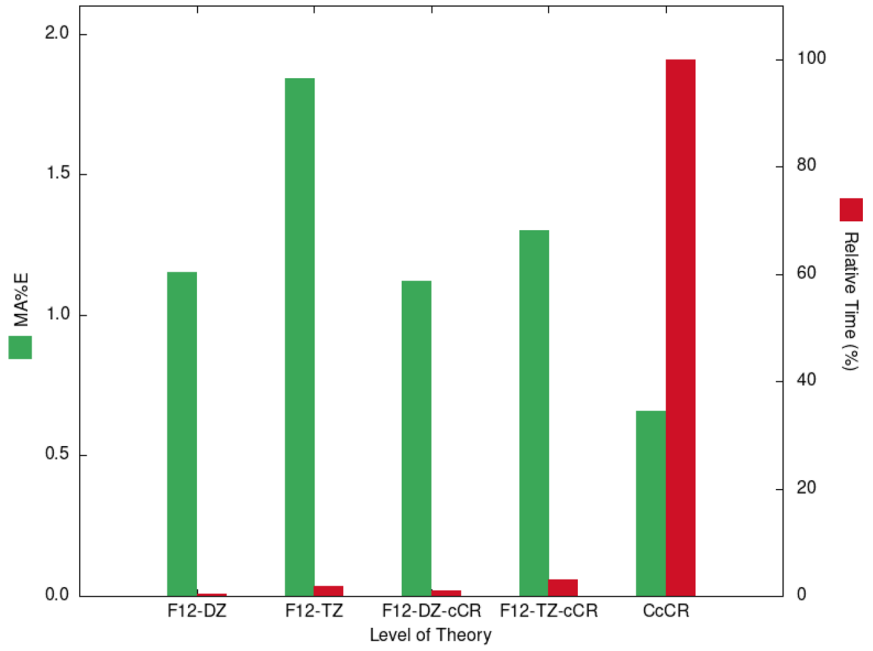

Figure 2. MA%E in the fundamental vibrational frequencies and timing.

accurate data are of the utmost necessity to aid the analysis of infrared and vibrational spectroscopic data from NASA missions like the ongoing SOFIA mission and the upcoming JWST.

■ ASSOCIATED CONTENT

Supporting Information

The Supporting Information is available free of charge at https://pubs.acs.org/doi/10.1021/acs.jpca.1c08355.

Full sets of harmonic and anharmonic vibrational frequencies (PDF)

■ AUTHOR INFORMATION

Corresponding Author

Ryan C. Fortenberry − *Department of Chemistry & Biochemistry, University of Mississippi, University, Mississippi 38677-1848, United States;* orcid.org/0000-0003-4716-8225; Email: r410@olemiss.edu

Authors

Alexandria G. Watrous − *Department of Chemistry & Biochemistry, University of Mississippi, University, Mississippi 38677-1848, United States*

Brent R. Westbrook − *Department of Chemistry & Biochemistry, University of Mississippi, University, Mississippi 38677-1848, United States;* orcid.org/0000-0002-6878-0192

Complete contact information is available at: https://pubs.acs.org/10.1021/acs.jpca.1c08355

Notes

The authors declare no competing financial interest.

■ ACKNOWLEDGMENTS

This work was financially supported by NASA Grant NNX17AH15G (80NSSC20K0001), NSF Grant OIA-1757220, and the College of Liberal Arts at the University of Mississippi. The computational resources were provided by the Mississippi Center for Supercomputing Research (MCSR). Dr. Timothy J. Lee of the NASA Ames Research Center is acknowledged for comments, support, and encouragement for this and related work.

■ REFERENCES

(1) McCoy, A. B. Diffusion Monte Carlo Approaches for Investigating the Structure and Vibrational Spectra of Fluxional Systems. *Int. Rev. Phys. Chem.* **2006**, *25*, 77−107.

(2) Hill, J. G.; Mitrushchenkov, A.; Yousaf, K. E.; Peterson, K. A. Accurate *ab initio* Ro-vibronic Spectroscopy of the $\tilde{X}^2\Pi$ CCN Radical Using Explicitly Correlated Methods. *J. Chem. Phys.* **2011**, *135*, 144309.

(3) Bloino, J.; Barone, V. A Second-Order Perturbation Theory Route to Vibrational Averages and Transition Properties of Molecules: General Formulation and Application to Infrared and Vibrational Circular Dichroism Spectroscopies. *J. Chem. Phys.* **2012**, *136*, 124108.

(4) Carter, S.; Bowman, J. M.; Handy, N. C. Multimode Calculations of Rovibrational Energies of C_2H_4 and C_2D_4. *Mol. Phys.* **2012**, *110*, 775−781.

(5) Barone, V.; Biczysko, M.; Puzzarini, C. Quantum Chemistry Meets Spectroscopy for Astrochemistry: Increasing Complexity toward Prebiotic Molecules. *Acc. Chem. Res.* **2015**, *48*, 1413−1422.

(6) Puzzarini, C.; Barone, V. Diving for Accurate Structures in the Ocean of Molecular Systems with the Help of Spectroscopy and Quantum Chemistry. *Acc. Chem. Res.* **2018**, *51*, 548−556.

(7) Watson, J. K. G. In *Vibrational Spectra and Structure*; During, J. R., Ed.; Elsevier: Amsterdam, 1977; pp 1−89.

(8) Papousek, D.; Aliev, M. R. *Molecular Vibration-Rotation Spectra*; Elsevier: Amsterdam, 1982.

(9) Franke, P. R.; Stanton, J. F.; Douberly, G. E. How to VPT2: Accurate and Intuitive Simulations of CH Stretching Infrared Spectra Using VPT2+K with Large Effective Hamiltonian Resonance Treatments. *J. Phys. Chem. A* **2021**, *125*, 1301−1324.

(10) Fortenberry, R. C.; Lee, T. J. Computational Vibrational Spectroscopy for the Detection of Molecules in Space. *Annu. Rep. Comput. Chem.* **2019**, *15*, 173−202.

(11) Raghavachari, K.; Trucks, G. W.; Pople, J. A.; Head-Gordon, M. A Fifth-Order Perturbation Comparison of Electron Correlation Theories. *Chem. Phys. Lett.* **1989**, *157*, 479−483.
(12) Shavitt, I.; Bartlett, R. J. *Many-Body Methods in Chemistry and Physics: MBPT and Coupled-Cluster Theory*; Cambridge University Press: Cambridge, 2009.
(13) Crawford, T. D.; Schaefer, III, H. F. In *Reviews in Computational Chemistry*; Lipkowitz, K. B., Boyd, D. B., Eds.; Wiley: New York, 2000; Vol. *14*, pp 33−136.
(14) Fortenberry, R. C.; Huang, X.; Francisco, J. S.; Crawford, T. D.; Lee, T. J. The *trans*-HOCO Radical: Fundamental Vibrational Frequencies, Quartic Force Fields, and Spectroscopic constants. *J. Chem. Phys.* **2011**, *135*, 134301.
(15) Dunning, T. H. Gaussian Basis Sets for Use in Correlated Molecular Calculations. I. The Atoms Boron through Neon and Hydrogen. *J. Chem. Phys.* **1989**, *90*, 1007−1023.
(16) Kendall, R. A.; Dunning, T. H.; Harrison, R. J. Electron Affinities of the First-Row Atoms Revisited. Systematic Basis Sets and Wave Functions. *J. Chem. Phys.* **1992**, *96*, 6796−6806.
(17) Peterson, K. A.; Dunning, T. H. Benchmark Calculations with Correlated Molecular Wave Functions. VII. Binding Energy and Structure of the HF Dimer. *J. Chem. Phys.* **1995**, *102*, 2032−2041.
(18) Martin, J. M. L.; Lee, T. J. The Atomization Energy and Proton Affinity of NH_3. An *Ab Initio* Calibration Study. *Chem. Phys. Lett.* **1996**, *258*, 136−143.
(19) Martin, J. M. L.; Taylor, P. R. Basis Set Convergence for Geometry and Harmonic Frequencies. Are *h* Functions Enough? *Chem. Phys. Lett.* **1994**, *225*, 473−479.
(20) Douglas, M.; Kroll, N. Quantum Electrodynamical Corrections to the Fine Structure of Helium. *Ann. Phys.* **1974**, *82*, 89−155.
(21) Jansen, G.; Hess, B. A. Revision of the Douglas-Kroll Hamiltonian. *Phys. Rev. A: At., Mol., Opt. Phys.* **1989**, *39*, 6016−6017.
(22) de Jong, W. A.; Harrison, R. J.; Dixon, D. A. Parallel Douglas-Kroll Energy and Gradients in NWChem: Estimating Scalar Relativistic Effects Using Douglas-Kroll Contracted Basis Sets. *J. Chem. Phys.* **2001**, *114*, 48−53.
(23) Huang, X.; Taylor, P. R.; Lee, T. J. Highly Accurate Quartic Force Field, Vibrational Frequencies, and Spectroscopic Constants for Cyclic and Linear $C_3H_3^+$. *J. Phys. Chem. A* **2011**, *115*, 5005−5016.
(24) Fortenberry, R. C.; Huang, X.; Francisco, J. S.; Crawford, T. D.; Lee, T. J. Quartic Force Field Predictions of the Fundamental Vibrational Frequencies and Spectroscopic Constants of the Cations $HOCO^+$ and $DOCO^+$. *J. Chem. Phys.* **2012**, *136*, 234309.
(25) Fortenberry, R. C.; Huang, X.; Francisco, J. S.; Crawford, T. D.; Lee, T. J. Fundamental Vibrational Frequencies and Spectroscopic Constants of $HOCS^+$, $HSCO^+$, and Isotopologues via Quartic Force Fields. *J. Phys. Chem. A* **2012**, *116*, 9582−9590.
(26) Zhao, D.; Doney, K. D.; Linnartz, H. Laboratory Gas-Phase Detection of the Cyclopropenyl Cation (c−$C_3H_3^+$). *Astrophys. J., Lett.* **2014**, *791*, L28.
(27) Morgan, W. J.; Fortenberry, R. C. Quartic Force Fields for Excited Electronic States: Rovibronic Reference Data for the 1 $^2A'$ and 1 $^2A''$ States of the Isoformyl Radical, HOC. *Spectrochim. Acta, Part A* **2015**, *135*, 965−972.
(28) Theis, R. A.; Fortenberry, R. C. Potential Interstellar Noble Gas Molecules: $ArOH^+$ and $NeOH^+$ Rovibrational Analysis from Quantum Chemical Quartic Force Fields. *Mol. Astrophys.* **2016**, *2*, 18−24.
(29) Bizzocchi, L.; Lattanzi, V.; Laas, J.; Spezzano, S.; Giuliano, B. M.; Prudenzano, D.; Endres, C.; Sipilä, O.; Caselli, P. Accurate Sub-Millimetre Rest Frequencies for $HOCO^+$ and $DOCO^+$ Ions. *Astron. Astrophys.* **2017**, *602*, A34.
(30) Kitchens, M. J. R.; Fortenberry, R. C. The Rovibrational Nature of Closed-Shell Third-Row Triatomics: HOX and HXO, X = Si^+, P, S^+, and Cl. *Chem. Phys.* **2016**, *472*, 119−127.
(31) Fortenberry, R. C.; Francisco, J. S. On the Detectability of the $\tilde{X}^2A''$ HSS, HSO, and HOS Radicals in the Interstellar Medium. *Astrophys. J.* **2017**, *835*, 243.
(32) Fuente, A.; Goicoechea, J. R.; Pety, J.; Gal, R. L.; Martín-Doménech, R.; Gratier, P.; Guzmán, V.; Roueff, E.; Loison, J. C.; Caro, G. M. M.; et al. First Detection of Interstellar S_2H. *Astrophys. J., Lett.* **2017**, *851*, 49.
(33) Wagner, J. P.; McDonald, D. C., II; Duncan, M. A. An Argon−Oxygen Covalent Bond in the $ArOH^+$ Molecular Ion. *Angew. Chem., Int. Ed.* **2018**, *57*, 5081−5085.
(34) Gardner, M. B.; Westbrook, B. R.; Fortenberry, R. C.; Lee, T. J. Highly-Accurate Quartic Force Fields for the Prediction of Anharmonic Rotational Constants and Fundamental Vibrational Frequencies. *Spectrochim. Acta, Part A* **2021**, *248*, 119184.
(35) Adler, T. B.; Knizia, G.; Werner, H.-J. A Simple and Efficient CCSD(T)-F12 Approximation. *J. Chem. Phys.* **2007**, *127*, 221106.
(36) Knizia, G.; Adler, T. B.; Werner, H.-J. Simplified CCSD(T)-F12 Methods: Theory and Benchmarks. *J. Chem. Phys.* **2009**, *130*, 054104.
(37) Peterson, K. A.; Adler, T. B.; Werner, H.-J. Systematically Convergent Basis Sets for Explicitly Correlated Wavefunctions: The Atoms H, He, B-Ne, and Al-Ar. *J. Chem. Phys.* **2008**, *128*, 084102.
(38) Yousaf, K. E.; Peterson, K. A. Optimized Auxiliary Basis Sets for Explicitly Correlated Methods. *J. Chem. Phys.* **2008**, *129*, 184108.
(39) Huang, X.; Valeev, E. F.; Lee, T. J. Comparison of One-Particle Basis Set Extrapolation to Explicitly Correlated Methods for the Calculation of Accurate Quartic Force Fields, Vibrational Frequencies, and Spectroscopic Constants: Application to H_2O, N_2H^+, NO_2^+, and C_2H_2. *J. Chem. Phys.* **2010**, *133*, 244108.
(40) Hill, J. G.; Mazumder, S.; Peterson, K. A. Correlation Consistent Basis Sets for Molecular Core-Valence Effects with Explicitly Correlated Wave Functions: The Atoms B-Ne and Al-Ar. *J. Chem. Phys.* **2010**, *132*, 054108.
(41) Martin, J. M. L.; Kesharwani, M. K. Assessment of CCSD(T)-F12 Approximations and Basis Sets for Harmonic Vibrational Frequencies. *J. Chem. Theory Comput.* **2014**, *10*, 2085−2090.
(42) Westbrook, B. R.; Valencia, E. M.; Rushing, S. C.; Tschumper, G. S.; Fortenberry, R. C. Anharmonic Vibrational Frequencies of Ammonia Borane (BH_3NH_3). *J. Chem. Phys.* **2021**, *154*, 041104.
(43) Agbaglo, D.; Lee, T. J.; Thackston, R.; Fortenberry, R. C. A Small Molecule with PAH Vibrational Properties and a Detectable Rotational Spectrum: *c*-(C)C_3H_2, Cyclopropenylidenyl Carbene. *Astrophys. J.* **2019**, *871*, 236.
(44) Watts, J. D.; Gauss, J.; Bartlett, R. J. Coupled-Cluster Methods with Noniterative Triple Excitations for Restricted Open-Shell Hartree-Fock and Other General Single Determinant Reference Functions. Energies and Analytical Gradients. *J. Chem. Phys.* **1993**, *98*, 8718−8733.
(45) Hill, J. G.; Peterson, K. A. Correlation Consistent Basis Sets for Explicitly Correlated Wavefunctions: Valence and Core-Valence Basis Sets for Li, Be, Na, and Mg. *Phys. Chem. Chem. Phys.* **2010**, *12*, 10460−10468.
(46) Werner, H.-J.; Knowles, P. J.; Manby, F. R.; Black, J. A.; Doll, K.; Heßelmann, A.; Kats, D.; Köhn, A.; Korona, T.; Kreplin, D. A.; et al. *MOLPRO*, Ver. 2020.1, a Package of *ab Initio* Programs, 2020; see http://www.molpro.net.
(47) Thackston, R.; Fortenberry, R. C. An Efficient Algorithm for the Determination of Force Constants and Displacements in Numerical Definitions of a Large, General Order Taylor Series Expansion. *J. Math. Chem.* **2018**, *56*, 103−119.
(48) Allen, W. D.; Császár, A. G.; Szalay, V.; Mills, I. M.; Horner, D. A. *INTDER 2005 is a General Program Written by W. D. Allen and Coworkers, which Performs Vibrational Analysis and Higher-Order Non-Linear Transformations*, 2005.
(49) Gaw, J. F.; Willets, A.; Green, W. H.; Handy, N. C. *SPECTRO program*, ver. 3.0, 1996.
(50) Mills, I. M. In *Molecular Spectroscopy - Modern Research*; Rao, K. N., Mathews, C. W., Eds.; Academic Press: New York, 1972; pp 115−140.
(51) Martin, J. M. L.; Taylor, P. R. Accurate *ab Initio* Quartic Force Field for *trans*-HNNH and Treatment of Resonance Polyads. *Spectrochim. Acta, Part A* **1997**, *53*, 1039−1050.

https://doi.org/10.1021/acs.jpca.1c08355
J. Phys. Chem. A 2021, 125, 10532−10540

(52) Martin, J. M. L.; Lee, T. J.; Taylor, P. R.; François, J.-P. The Anharmonic Force Field of Ethylene, C_2H_4, by Means of Accurate *ab Initio* Calculations. *J. Chem. Phys.* **1995**, *103*, 2589−2602.
(53) Lee, T. J.; Fortenberry, R. C. The Unsolved Issue with Out-of-Plane Bending Frequencies for C = C Multiply Bonded Systems. *Spectrochim. Acta, Part A* **2021**, *248*, 119148.
(54) Brunken, S.; Gottlieb, C. A.; Gupta, H.; McCarthy, M. C.; Thaddeus, P. Laboratory Detection of the Negative Molecular Ion CCH^-. *Astron. Astrophys.* **2007**, *464*, L33−L36.
(55) Shimanouchi, T. *Tables of Molecular Vibrational Frequencies*, 39th ed.; National Standards Reference Data System: Washington, DC, 1972; Vol. *1*.
(56) Brünken, S.; Müller, H. S. P.; Lewen, F.; Winnewisser, G. High Accuracy Measurements on the Ground State Rotational Spectrum of Formaldehyde (H_2CO) up to 2 THz. *Phys. Chem. Chem. Phys.* **2003**, *5*, 1515−1518.
(57) Tennyson, J.; Zobov, N. F.; Williamson, R.; Polyansky, O. L.; Bernath, P. F. Experimental Energy Levels of the Water Molecule. *J. Phys. Chem. Ref. Data* **2001**, *30*, 735.
(58) De Lucia, F. C.; Helminger, P.; Cook, R. L.; Gordy, W. Submillimeter Microwave Spectrum of $H_2{}^{16}O$. *Phys. Rev. A: At., Mol., Opt. Phys.* **1972**, *5*, 487−490.
(59) Mellau, G. C. Complete Experimental Rovibrational Eigenenergies of HNC up to 3743 cm^{-1} above the Ground State. *J. Chem. Phys.* **2011**, *134*, 234303.
(60) Amano, T. The ν_1 Fundamental Band of HCO^+ by Difference Frequency Laser Spectroscopy. *J. Chem. Phys.* **1983**, *79*, 3595.
(61) Foster, S. C.; McKellar, A. R. W.; Sears, T. J. Observation of the ν_3 Fundamental Band of HCO^+. *J. Chem. Phys.* **1984**, *81*, 578.
(62) Davies, P. B.; Hamilton, P. A.; Rothwell, W. J. Infrared Laser Spectroscopy of the ν_3 Fundamental of HCO^+. *J. Chem. Phys.* **1984**, *81*, 1598−1599.
(63) Cazzoli, G.; Cludi, L.; Buffa, G.; Puzzarini, C. Precise THz Measurements of HCO^+, N_2H^+, and CF^+ for Astrophysical Observations. *Astrophys. J., Suppl. Ser.* **2012**, *203*, 1−9.
(64) Cabezas, C.; Cernicharo, J.; Alonso, J. L.; Agúndez, M.; Mata, S.; Guélin, M.; Peña, I. Laboratory and Astronomical Discovery of Hydromagnesium Isocyanide. *Astrophys. J.* **2013**, *775*, 133.
(65) Mellau, G. C. The ν_1 Band System of HNC. *J. Mol. Spectrosc.* **2010**, *264*, 2−9.
(66) Johns, J. W. C.; McKellar, A. R. W.; Weinberger, E. The Infrared Spectrum of HNO. *Can. J. Phys.* **1983**, *61*, 1106−1119.
(67) Yoshikawa, T.; Watanabe, A.; Sumiyoshi, Y.; Endo, Y. Laser Spectroscopy of the $\tilde{A}^2A'-\tilde{X}^2A''$ System for the HSO Radical. *J. Mol. Spectrosc.* **2009**, *254*, 119−125.
(68) Cazzoli, G.; Lattanzi, V.; Kirsch, T.; Gauss, J.; Tercero, B.; Cernicharo, J.; Puzzarini, C. Laboratory Measurements and Astronomical Search for the HSO Radical. *Astron. Astrophys.* **2016**, *591*, A126.
(69) Ashworth, S. H.; Fink, E. H. The High Resolution Fourier-Transform Chemiluminescene Spectrum of the HS_2 Radical. *Mol. Phys.* **2007**, *105*, 715−725.
(70) Yamamoto, S.; Saito, S. Microwave Spectrum and Molecular Structure of the HS_2 Radical. *Can. J. Phys.* **1994**, *72*, 954−962.
(71) Jacox, M. E. Vibrational and Electronic Energy Levels of Polyatomic Transient Molecules. Supplement B. *J. Phys. Chem. Ref. Data* **2003**, *32*, 1−441.
(72) Brünken, S.; Gottlieb, C. A.; McCarthy, M. C.; Thaddeus, P. Laboratory Detection of HOCN and Tentative Identification in Sgr B2. *Astrophys. J.* **2009**, *697*, 880.
(73) Oyama, T.; Funato, W.; Sumiyoshi, Y.; Endo, Y. Observation of the Pure Rotational Spectra of *trans*- and *cis*-HOCO. *J. Chem. Phys.* **2011**, *134*, 174303.
(74) Petty, J. T.; Moore, C. B. Transient Infrared-Absorption Spectrum of the ν_1 Fundamental of *trans*-HOCO. *J. Mol. Spectrosc.* **1993**, *161*, 149−156.
(75) Amano, T.; Tanaka, K. Difference Frequency Laser Spectroscopy of the ν_1 Band of $HOCO^+$. *J. Chem. Phys.* **1985**, *82*, 1045−1046.
(76) Bogey, M.; Demuynck, C.; Destombes, J. L.; Krupnov, A. Molecular Structure of $HOCO^+$. *J. Mol. Struct.* **1988**, *190*, 465−474.
(77) Lattanzi, V.; Thorwirth, S.; Halfen, D. T.; Mück, L. A.; Ziurys, L. M.; Thaddeus, P.; Gauss, J.; McCarthy, M. C. Bonding in the Heavy Analogue of Hydrogen Cyanide: The Curious Case of Bridged HPSi. *Angew. Chem., Int. Ed.* **2010**, *49*, 5661−5664.
(78) Tack, L. M.; Rosenbaum, N. H.; Owrutsky, J. C.; Saykally, R. J. Velocity Modulation Infrared Laser Spectroscopy and Structure of the Amide Anion (NH_2^-). *J. Chem. Phys.* **1986**, *85*, 4222−4227.
(79) Dowling, J. M. The Rotation-Inversion Spectrum of Ammonia. *J. Mol. Spectrosc.* **1968**, *27*, 527−538.
(80) Benedict, W. S.; Plyler, E. K.; Tidwell, E. D. Vibration-Rotation Bands of Ammonia: 1. The Combination Bands $\nu_2 + (\nu_1, \nu_3)$. *J. Res. Natl. Inst. Stand. Technol.* **1958**, *61*, 123−147.
(81) Amano, T. Spectroscopic Detection of Protonated N_2O. *Chem. Phys. Lett.* **1986**, *127*, 101−104.
(82) Bogey, M.; Demuynck, C.; Destombes, J. L. Millimeter and Submillimeter Wave Spectroscopy of Protonated and Deuterated Nitrous Oxide. *J. Chem. Phys.* **1988**, *88*, 2108−2111.
(83) Hirahara, Y.; Masuda, A.; Kawaguchi, K. Fourier Transform Infrared Spectroscopy of the ν_3 Band of Cyclopropenylidene, C_3H_2. *J. Chem. Phys.* **1991**, *95*, 3975−3979.
(84) Thaddeus, P.; Gottlieb, C. A.; Hjalmarson, A.; Johansson, L. E. B.; Irvine, W. M.; Friberg, P.; Linke, R. A. Astronomical Detection of the C_3H Radical. *Astrophys. J.* **1985**, *294*, L49−L53.
(85) Westbrook, B. R.; Del Rio, W. A.; Lee, T. J.; Fortenberry, R. C. Overcoming the Out-of-plane Bending Issue in an Aromatic Hydrocarbon: The Anharmonic Vibrational Frequencies of c-$(CH)C_3H_2^+$. *Phys. Chem. Chem. Phys.* **2020**, *22*, 12951−12958.
(86) Huang, X.; Lee, T. J. Accurate *Ab Initio* Quartic Force Fields for NH_2^- and CCH^- and Rovibrational Spectroscopic Constants for Their Isotopologs. *J. Chem. Phys.* **2009**, *131*, 104301.
(87) Valencia, E. M.; Worth, C. J.; Fortenberry, R. C. Enstatite ($MgSiO_3$) and Forsterite (Mg_2SiO_4) Monomers and Dimers: Highly-Detectable Infrared and Radioastronomical Molecular Building Blocks. *Mon. Not. R. Astron. Soc.* **2020**, *492*, 276−282.
(88) Mackie, C. J.; Candian, A.; Huang, X.; Maltseva, E.; Petrignani, A.; Oomens, J.; Buma, W. J.; Lee, T. J.; Tielens, A. G. G. M. The Anharmonic Quartic Force Field Infrared Spectra of Three Polycyclic Aromatic Hydrocarbons: Naphthalene, Anthracene, and Tetracene. *J. Chem. Phys.* **2015**, *143*, 224314.

https://doi.org/10.1021/acs.jpca.1c08355
J. Phys. Chem. A 2021, 125, 10532−10540